Molecular Therapy
Original Article

m^{6}A RNA hypermethylation-induced BACE2 boosts intracellular calcium release and accelerates tumorigenesis of ocular melanoma

Fanglin He,[1,2,3] Jie Yu,[1,2,3] Jie Yang,[1,2,3] Shaoyun Wang,[1,2] Ai Zhuang,[1,2] Hanhan Shi,[1,2] Xiang Gu,[1,2] Xiaofang Xu,[1,2] Peiwei Chai,[1,2] and Renbing Jia[1,2]

[1]Department of Ophthalmology, Shanghai Ninth People's Hospital, Shanghai Jiao Tong University School of Medicine, Shanghai 200001, China; [2]Shanghai Key Laboratory of Orbital Diseases and Ocular Oncology, Shanghai 200001, China

Ocular melanoma, including uveal melanoma (UM) and conjunctival melanoma (CM), is the most common and deadly eye cancer in adults. Both UM and CM originate from melanocytes and exhibit an aggressive growth pattern with high rates of metastasis and mortality. The integral membrane glycoprotein beta-secretase 2 (BACE2), an enzyme that cleaves amyloid precursor protein into amyloid beta peptide, has been reported to play a vital role in vertebrate pigmentation and metastatic melanoma. However, the role of BACE2 in ocular melanoma remains unclear. In this study, we showed that BACE2 was significantly upregulated in ocular melanoma, and inhibition of BACE2 significantly impaired tumor progression both *in vitro* and *in vivo*. Notably, we identified that transmembrane protein 38B (TMEM38B), whose expression was highly dependent on BACE2, modulated calcium release from endoplasmic reticulum (ER). Inhibition of the BACE2/TMEM38B axis could trigger exhaustion of intracellular calcium release and inhibit tumor progression. We further demonstrated that BACE2 presented an increased level of N^6-methyladenosine (m^{6}A) RNA methylation, which led to the upregulation of BACE2 mRNA. To our knowledge, this study provides a novel pattern of BACE2-mediated intracellular calcium release in ocular melanoma progression, and our findings suggest that m^{6}A/BACE2/TMEM38b could be a potential therapeutic axis for ocular melanoma.

INTRODUCTION

Ocular melanoma, which mainly includes uveal melanoma (UM) and conjunctival melanoma (CM), is the most common eye cancer in adults and the second most common melanoma, with a high rate of recurrence and an unfavorable prognosis.[1] About 80% of UM patients harbor activating mutations in G protein subunit alpha Q (*GNAQ*) or G protein subunit alpha 11 (*GNA11*),[2] which could activate YAP, resulting in promotion of cell proliferation and sensitization of cells to mitogen-activated protein kinase (MAPK) inhibitors.[3,4] In addition, the loss of chromosome 3 has been frequently identified in UM. Notably, CM is epidemiologically, molecularly, and genetically different from UM.[5] To date, the mechanism of CM remains inclusive, and some researchers have suggested that the mechanism of CM oncogenesis is similar to that of skin cutaneous melanoma (SKCM), which has been reported to be highly involved in immune invasion.[6] Successful anti-PD1 immunotherapy for five patients with metastatic CM with up to 36 months of follow-up has been reported.[7]

Recently, epigenetic drivers of ocular melanoma have been reported to play important roles in tumorigenesis of ocular melanoma, including DNA methylation, histone modifications, long non-coding RNAs (lncRNAs), and N^6-methyladenosine (m^{6}A) RNA methylation.[7] For example, lncRNA ROR serves as a decoy oncogenic RNA (oncoRNA) that blocks G9a (a key enzyme of histone H3K9 methylation) binding to the promoters of *TESC*s, thereby enhancing UM tumorigenesis.[8] Notably, m^{6}A RNA methylation has been revealed to inhibit ocular melanoma progression by translational activation of *HINT2*, a tumor suppressor gene.[7] In addition, a three-m^{6}A regulators signature (ALKBH5, YTHDF1, and KIAA1429) for UM was established as a new promising biomarker for prognosis and treatment strategy development.[9] However, the mechanism of ocular melanoma tumorigenesis requires further exploration.

Beta-secretase 2 (*BACE2*), which encodes an integral membrane glycoprotein that functions as an aspartic protease, cleaves amyloid precursor protein into amyloid beta peptide, which is a critical step in the etiology of Alzheimer's disease and Down syndrome.[10] *BACE2* contributes to AD pathogenesis as a conditional β-secretase and could be a preventive and therapeutic target for AD without side effects of BACE1 inhibition.[11] In addition, BACE2 has been reported to be involved in melanosome amyloid matrix formation in

Received 10 November 2020; accepted 10 February 2021;
https://doi.org/10.1016/j.ymthe.2021.02.014.

[3]These authors contributed equally

Correspondence: Renbing Jia, MD, PhD, Department of Ophthalmology, Shanghai Ninth People's Hospital, Shanghai Jiao Tong University School of Medicine, Shanghai 200025, China.
E-mail: renbingjia@sjtu.edu.cn

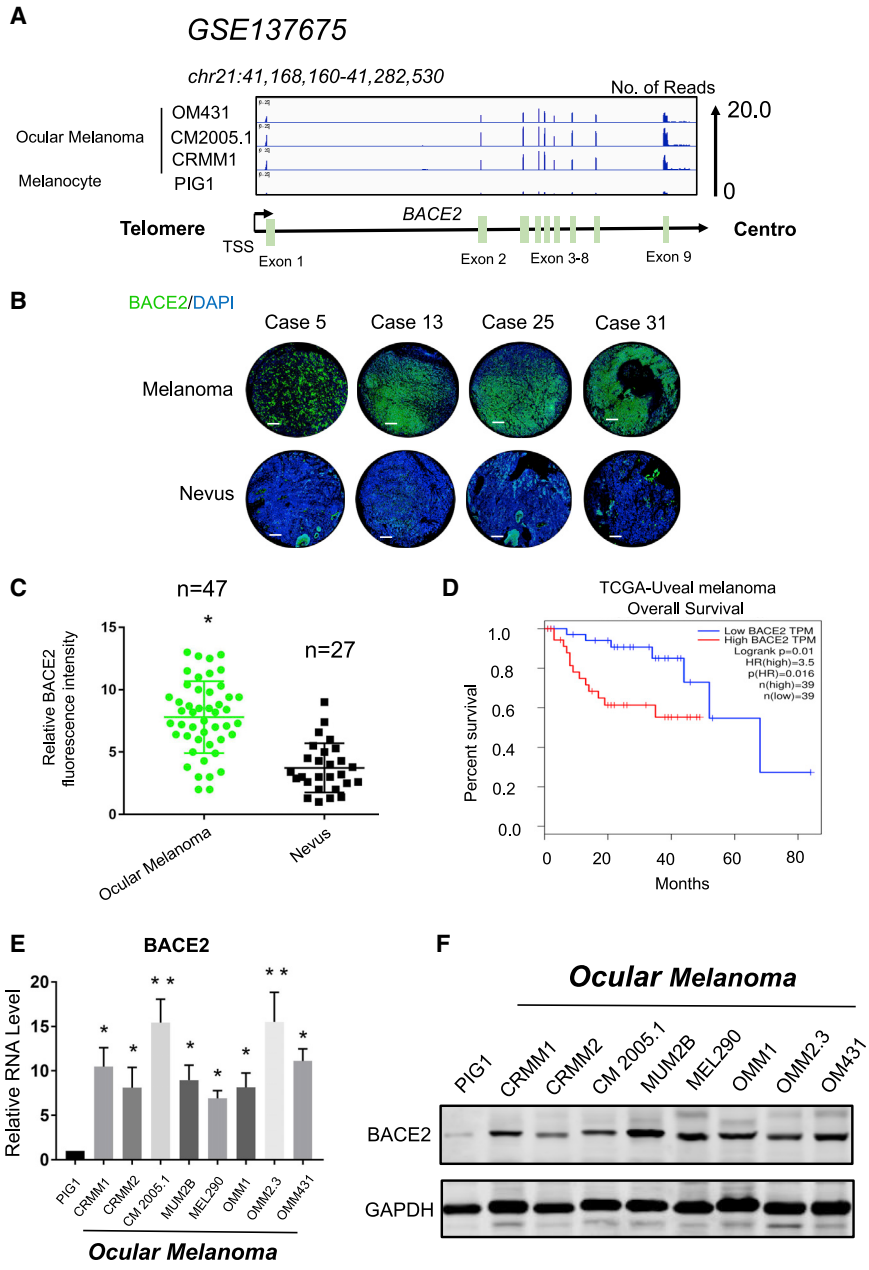

Figure 1. The expression and prognostic value of BACE2 in ocular melanoma

(A) RNA sequencing analysis was performed to evaluate the transcriptome of uveal melanoma (OM431) and conjunctival melanoma (CRMM1, CM2005.1) cell lines. Green chart: the exons of BACE2. (B and C) BACE2 expression according to IF analysis (B) and statistical results of BACE2 expression in normal and tumor tissues (C). Scale bars, 100 μm. (D) Kaplan-Meier analysis of the correlations between BACE2 expression and overall survival in the internal cohort (n = 39, p = 0.01). (E) Real-time PCR was performed to show the BACE2 expression levels in ocular melanoma cells. *p < 0.05, **p < 0.01. (F) Western blot showing the protein levels of BACE2 in the tumor and normal cells. GAPDH was used as an internal control.

pigment cells.[12] However, the role of BACE2 in tumorigenesis, especially in ocular melanoma, remains unclear.

We thus aimed to identify the molecular mechanisms and potential clinical application of BACE2 in ocular melanoma. In this study, we revealed for the first time that BACE2 was significantly upregulated in ocular melanoma. In addition, target correction of the BACE2/transmembrane protein 38B (TMEM38B) axis triggered exhaustion of intracellular calcium release and inhibited tumor progression. Our findings suggest that BACE2 could be a potential therapeutic target for ocular melanoma.

RESULTS

BACE2 was upregulated in ocular melanoma

To explore candidate genes in tumorigenesis of ocular melanoma, we analyzed RNA sequencing (RNA-seq) data of both ocular melanoma cells and normal control cells (GEO: GSE137675). We found that BACE2 was significantly upregulated in both UM (OM431) and CM (CRMM1, CM2005.1) cell lines (Figure 1A). We next examined BACE2 expression in ocular melanoma samples using a tissue chip (Table S2), and a significant upregulation of BACE2 expression was noted in ocular melanoma samples (Figures 1B and 1C). Accordingly, we queried both The Cancer Genome Atlas (TCGA) database and the Genotype-Tissue Expression (GTEx) database for bioinformatics assays, with GTEx providing normal control data of melanoma through GEPIA (http://gepia.cancer-pku.cn),[13] and we found that BACE2 was significantly upregulated in melanoma tissues ($p < 0.05$, Figure S1A). Moreover, we found that increased BACE2 expression (log-rank p = 0.01) referred to an unfavorable overall outcome for ocular melanoma patients in TCGA database (Figure 1D). In parallel, for disease-free survival data, elevated expression of BACE2 (log-rank p = 0.058) presented with a possible trend of a larger proportion of recurrence in ocular melanoma (Figure S1B). In addition, BACE2 was upregulated in most ocular melanoma cell lines at both the mRNA (Figure 1E) and protein (Figures 1F and S1C) levels.

Inhibition of BACE2 showed therapeutic efficacy in ocular melanoma *in vitro* and *in vivo*

We then explored whether silencing BACE2 could attenuate tumor proliferation and metastasis. First, we designed two small hairpin RNAs (shRNAs) (shBACE2-1 and shBACE2-2, with an EGPF tag) for

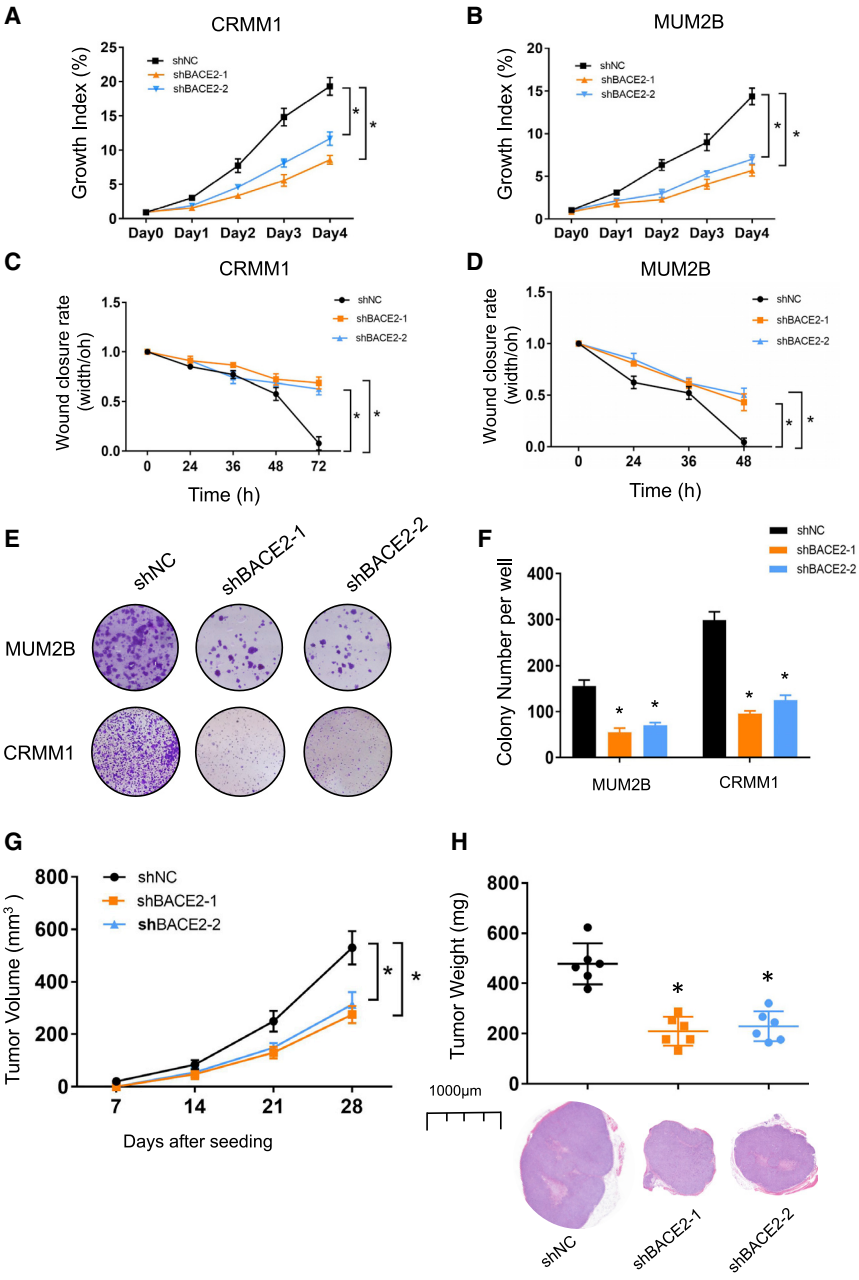

Figure 2. BACE2 inhibits ocular melanoma growth *in vitro* and *in vivo*

(A and B) A CCK-8 assay was performed to measure tumor cell growth after BACE2 knockdown, *p < 0.05 compared with the control. (C and D) Wound-healing assay results demonstrate tumor migration. The results are expressed as the ratio of the current width to the original scratch width. *p < 0.05 compared with the control. (E) A colony formation assay was used to assess the cell growth rate of tumor cells treated with shRNA. (F) Small colonies on each plate were counted. All of the data are presented as the mean ± SEM. *p < 0.05, compared with the control. (G and H) After subcutaneous injection, the tumor sizes were measured weekly; the tumor growth rate (G) and tumor weight (H) on day 28 are shown. *p < 0.05, compared with the control groups, with three replicates. Representative images of H&E staining for the evaluation of tumor formation *in vivo* are shown. Scale bar, 1,000 μm (bottom).

silencing BACE2. Using EGFP as a tracking marker, we observed green fluorescence in the CRMM1 and MUM2B cell lines after lentivirus transfection (Figure S2A). As expected, BACE2 expression was reduced compared to that of control group at both the mRNA (Figure S2B) and protein (Figure S2C) levels. Importantly, we observed a significant inhibition of cell growth (Figures 2A and 2B) and migration (Figures 2C, 2D, S3A, and S3B) after silencing BACE2 in ocular melanoma cells. In addition, the BACE2-silenced ocular melanoma cells formed fewer and smaller colonies than did control cells (Figures 2E and 2F). To assess their tumor formation ability *in vivo*, we injected control and BACE2-silenced MUM2B melanoma cells into nude mice and monitored tumor growth. At day 28, detectable xenograft volume reached nearly 600 mm^3 in the control group; however, the volume of tumors was only about 300 mm^3 after silencing BACE2 by two individual shRNAs (Figures 2G and S4A, *p < 0.05). In addition, an approximately 80% decrease was noted in average weight of the xenografts in the BACE2-silenced group compared with control groups (Figure 2H, *p < 0.05). Additionally, a significantly decreased BACE2 fluorescence signal (488 nm, Figures S4B and S4C, *p < 0.05) and Ki67-positive rate were observed in BACE2-silenced xenografts (Figure S4D, *p < 0.05). Taken together, these experiments demonstrated that reprogrammed cells with corrected BACE2 exhibited markedly improved antitumor outcomes *in vitro* and *in vivo*.

Transcriptome screening identified TMEM38B as a downstream target of BACE2

We then explored the mechanism underlying ocular melanoma inhibition induced by BACE2 silencing. Through RNA-seq assays (GEO: GSE155530), we found 15 downregulated and 30 upregulated genes in the BACE2-inhibited group ($|\log_2$fold change [FC]$|$ > 1.5, p < 0.05, Figure 3A). Notably, BACE2 was the most downregulated gene (Figure 3B) and served as a positive control for RNA-seq assays. In addition, the BACE2-silenced group presented a distinct transcriptional pattern, which was substantially different from that of the control group (Figures S5A and S5B). Through gene set enrichment analysis (GSEA), we found that major genes in cation channel activity signaling pathways were downregulated (Figure 3C). Accordingly, through Circos

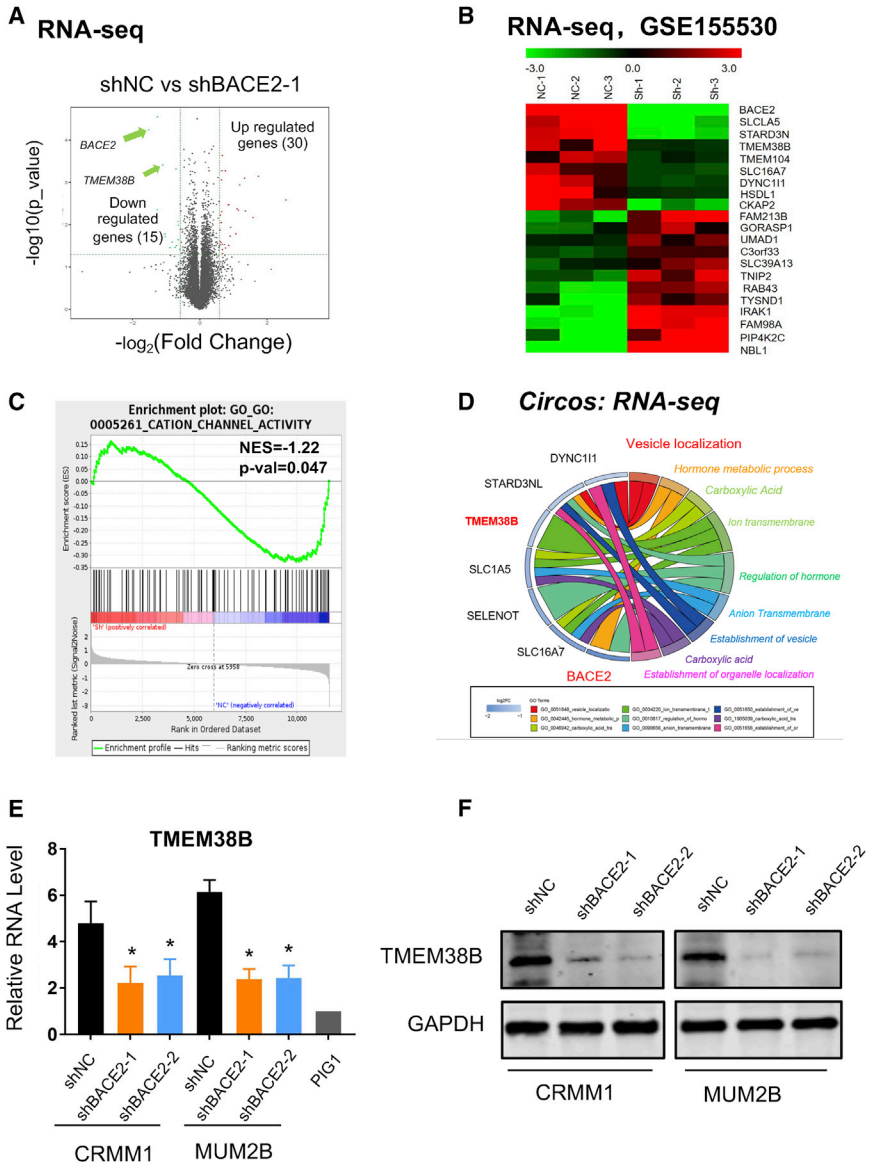

Figure 3. Transcriptome-wide identification of downstream targets of BACE2

(A) Volcano plots showing 15 downregulated and 30 upregulated genes in the BACE2-inhibited group (log_2FC| > 1.5, p < 0.05). (B) Heatmap of genes showing BACE2 was the most downregulated among them. (C) GSEA plots evaluating the major genes in cation channel activity signaling pathways after knocking down BACE2 (NES = −1.22, p = 0.047). (D) Circos analysis showing significantly downregulated genes in the BACE2-silenced cells and their related functions. (E) Real-time PCR was performed to show the TMEM38B expression levels in BACE2-silenced cells. (F) Western blot showing the protein levels of TMEM38B in the BACE2-silenced cells. GAPDH was used as an internal control.

analysis, we found that an important calcium channel protein, TMEM38B, was significantly downregulated in BACE2-silenced cells (Figure 3D). Furthermore, we confirmed that both mRNA (Figure 3E) and protein (Figures 3F, S4E, and S4F) levels of TMEM38B were significantly decreased after knocking down BACE2. To further illustrate that TMEM38B is the downstream target of BACE2, we next successfully inhibited TMEM38B expression by two individual shRNAs (Figures S6A and S6D). Moreover, in BACE2-silenced xenografts, we observed a significant reduction of TMEM38B fluorescence intensity (Figures S7A and S7B, *p < 0.05). More importantly, parallel expression of BACE2 and TMEM38B was also observed in TCGA melanoma samples (Figure S7C, p < 0.01, R = 0.21). We next overexpressed TMEM38B in both RNA (Figure S7D) and protein levels (Figure S7E, left panel, lanes 1 and 3) after cloning the full length of TMEM38B into a pcDNA3.1 vector. However, we did not observe a significant change of BACE2 expression after silencing TMEM38B or overexpressing TMEM38B in ocular melanoma cells (Figure S7E, right panel). The result suggested that TMEM38B is the downstream target of BACE2.

TMEM38B was upregulated in ocular melanoma and associated with unfavorable prognosis

Since TMEM38B may serve as a downstream candidate of BACE2, we next explored TMEM38B expression in ocular melanoma using a tissue chip. We expected TMEM38B expression to be significantly overexpressed in clinical ocular tumor samples (Figures 4A and 4B) and TCGA melanoma datasets (Figure S8A). More importantly, upregulated TMEM38B was associated with unfavorable overall survival (log-rank p = 0.038) and a trend of unfavorable disease-free survival (log-rank p = 0.06) in the UM dataset from TCGA (Figure 4C). Accordingly, TMEM38B was upregulated in ocular melanoma cells at both the RNA (Figure 4D) and protein (Figures 4E and S8B) levels.

TMEM38B contributed to tumor progression both *in vitro* and *in vivo*

To determine the role of TMEM38B in ocular melanoma tumorigenesis, we next silenced TMEM38B in ocular melanoma cells. Using EGFP as a tag, we observed green fluorescence in CRMM1 and MUM2B cell lines after lentivirus transfection (Figure S6A). In addition, TMEM38B expression was reduced compared to that of the control group at both the mRNA (Figures S6B and S6C) and protein (Figure S6D) levels. Importantly, cell growth was significantly inhibited after knocking down TMEM38B in ocular melanoma cell lines (Figures 5A and 5B). Moreover, the TMEM38B-silenced cells formed

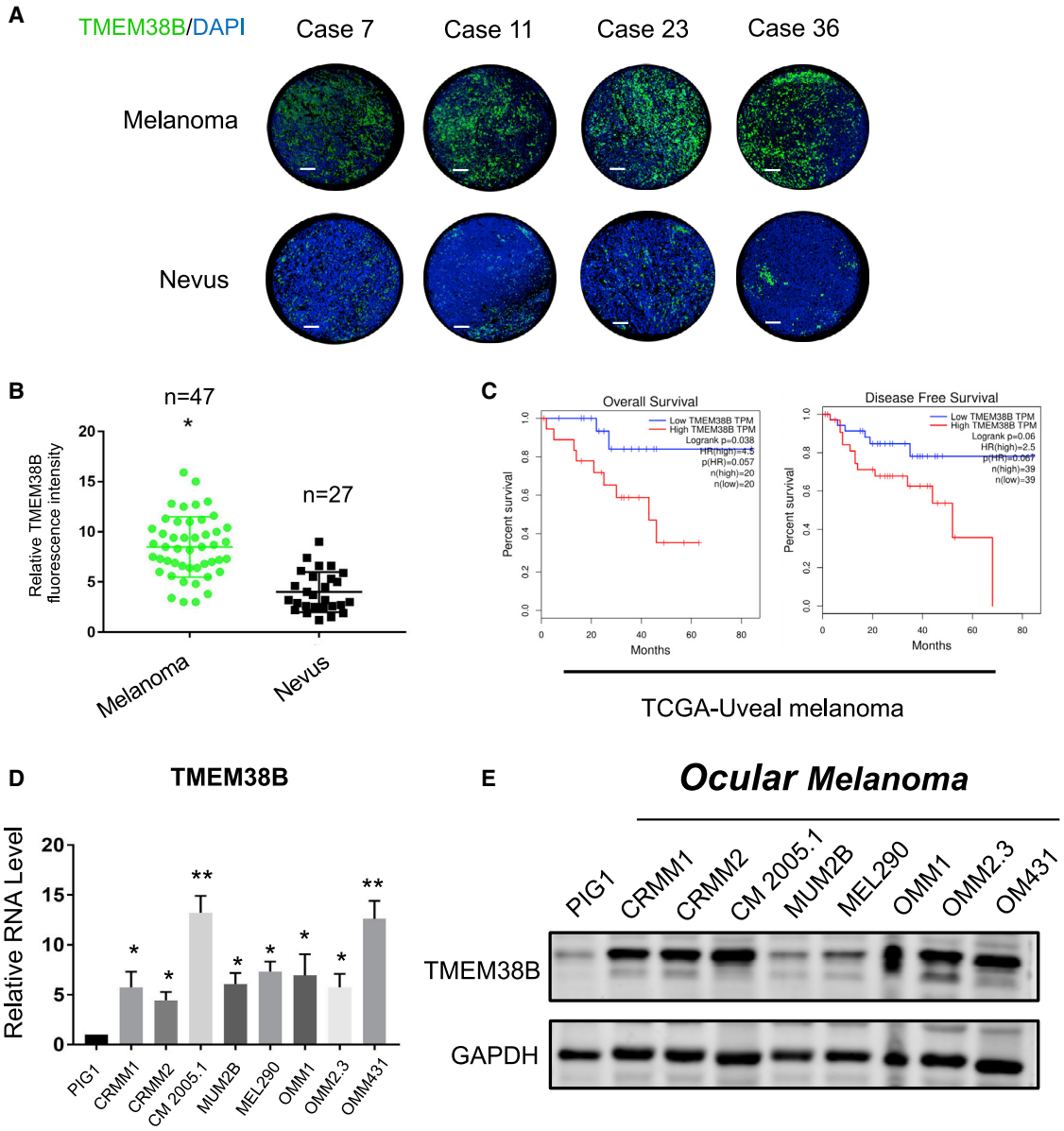

Figure 4. The expression and prognostic value of TMEM38B in ocular melanoma

(A and B) TMEM38B expression according to IF analysis (A) and statistical results of TMEM38B expression in normal and tumor tissues (B). Scale bars, 100 μm. (C) Kaplan-Meier analyses of the correlations between TMEM38B expression and overall survival or disease-free survival in the internal cohort. (D) Real-time PCR was performed to show TMEM38B expression levels in ocular melanoma cells. (E) Western blot showing the protein levels of TMEM38B in the tumor and normal cells. GAPDH was used as an internal control.

smaller and fewer colonies than did those of the empty control group (Figures 5C and 5D). To assess tumor formation *in vivo*, we then injected control and TMEM38B-silenced MUM2B melanoma cells into nude mice. As expected, TMEM38B-silenced tumor cells formed smaller xenografts than did control cells (Figures 5E, 5F, and S9A), with a decreased Ki67-positive rate (Figure S9B). Taken together, these data identified TMEM38B as an oncogene in the tumorigenesis of ocular melanoma.

TMEM38B modulated intracellular Ca^{2+} release in ocular melanoma

Since TMEM38B is an important protein in the maintenance of intracellular calcium release, we further tested intracellular Ca^{2+} abundance in BACE2/TMEM38B-silenced cells. Because the lentivirus carried an EGFP tag, which may interfere with the intracellular calcium release assay, we used two smalls interfering RNAs (siRNAs) to silence BACE2 and TMEM38B. These siRNAs shared a similar

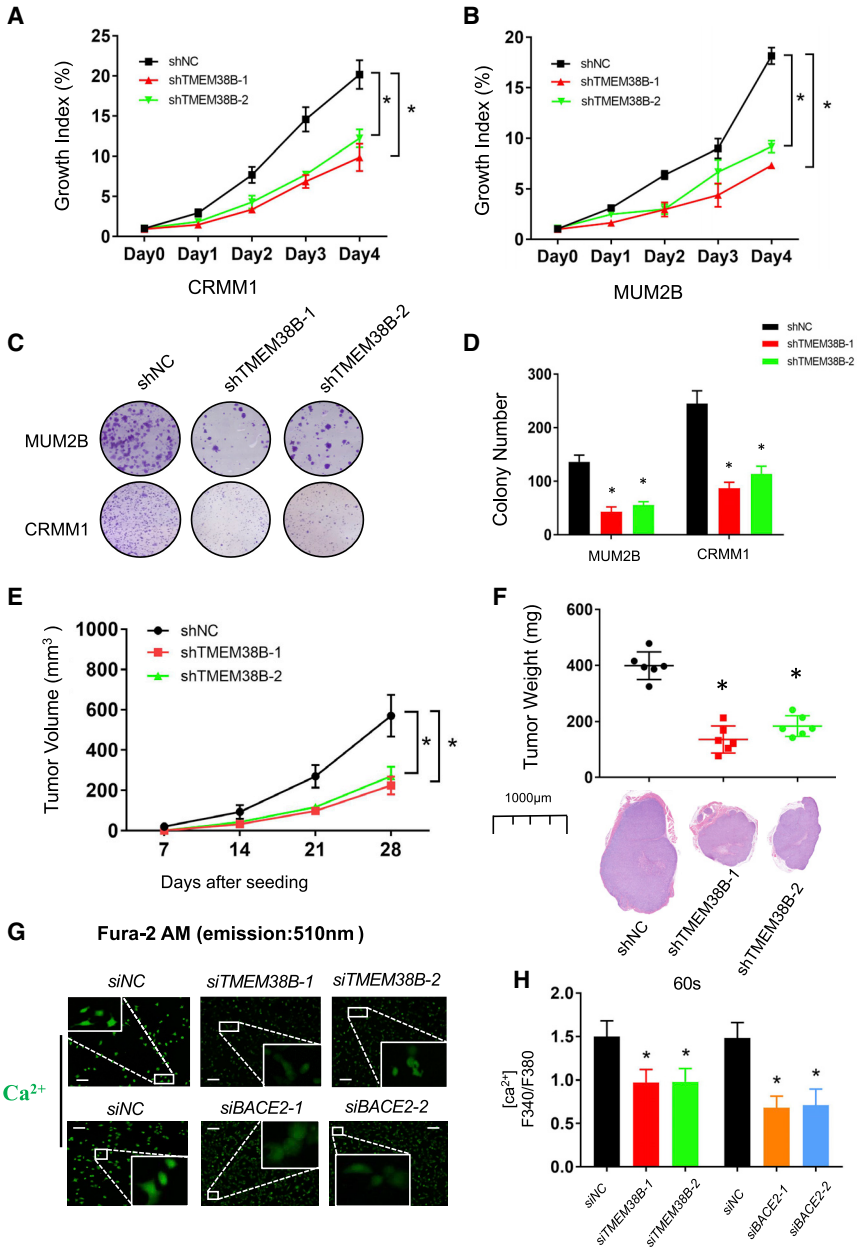

Figure 5. TMEM38B inhibits ocular melanoma growth and modulates Ca^{2+} flux in uveal melanoma

(A and B) CCK-8 assay showing that tumor cell growth was obviously restrained in the BACE2-silenced CRMM1 and MUM2B cells. *p < 0.05, compared with the control. (C) A colony formation assay was used to assess the cell growth rate of the tumor cells treated with shRNA. (D) Small colonies on each plate were counted. All the data are presented as the mean ± SEM. *p < 0.05, compared with the control. (E) After subcutaneous injection, the tumor sizes were measured weekly; the tumor growth rate (g) on day 28 is shown. *p < 0.05 with three replicates. (F) Top: the weight of the tumors was measured on day 28 after the tumors were surgically dissected. Bottom: representative images of H&E staining for the evaluation of tumor formation *in vivo*. Scale bar, 1,000 μm. (G) Intracellular calcium concentration was detected by a calcium fluorescence probe (fura-2-acetoxymethyl ester [fura-2 AM]) in the BACE2- and TMEM38b-deficient cells. (H) The intracellular Ca^{2+} abundance in the BACE2/TMEM38B-silenced cells at 60 s. *p < 0.05.

sequence with our short hairpin plasmid and exhibited efficient silencing of both BACE2 and TMEM38B (Figure S10A). More importantly, we also observed a significant decrease in intracellular calcium levels in BACE2- and TMEM38b-deficient cells (Figures 5F, 5G, and S10B). In addition, calmodulin is a widely expressed small protein that is considered to be the most important Ca^{2+} sensor in non-muscle cells. Increased Ca^{2+} in cytoplasm activates Ca^{2+}/calmodulin protein kinases to activate the phosphatidylinositol 3-kinase (PI3K)/Akt pathway, leading to an enhancement of tumor cell growth, metastasis, and epithelial-mesenchymal transition.[14] Herein, silencing TMEM38B significantly decreased phosphorylated (p-)calmodulin, whose level is influenced by intracellular calcium levels, and p-PI3K in parallel (Figure S10C). Taken together, these data indicated that TMEM38B may serve as an oncogenic driver by modulating calcium release, which is regulated by BACE2.

Reintroduction of TMEM38B rescued the Ca^{2+} influx and inhibitory phenotype in BACE2-depleted ocular melanoma cells

To verify whether reduced TMEM38B was responsible for suppressed Ca^{2+} influx and proliferation in BACE2-silenced melanoma cells, we aimed to reintroduce wild-type TMEM38B in BACE2-silenced cells to rescue the phenotype (Figures 6A and 6B). Accordingly, Ca^{2+} influx was reinforced after overexpressing TMEM38B in ocular melanomas (Figures 6C, 6D, and S11). Moreover, the reduced colony formation (Figure 6E) and migration (Figures 6F, S12A, and S12B) were neutralized after reintroducing TMEM38B in ocular melanoma. Conclusively, our study showed that TMEM38B is a critical candidate gene regulated by BACE2 and contributes to Ca^{2+} influx and tumor progression in ocular melanoma.

Excess m^6A RNA methylation participated in the overexpression of BACE2

We then explored the reason for the upregulation of BACE2 in ocular melanoma. Abundant studies have illuminated that m^6A RNA methylation is an important regulator of RNA splicing, degradation, and translational capacity. Through methylated RNA

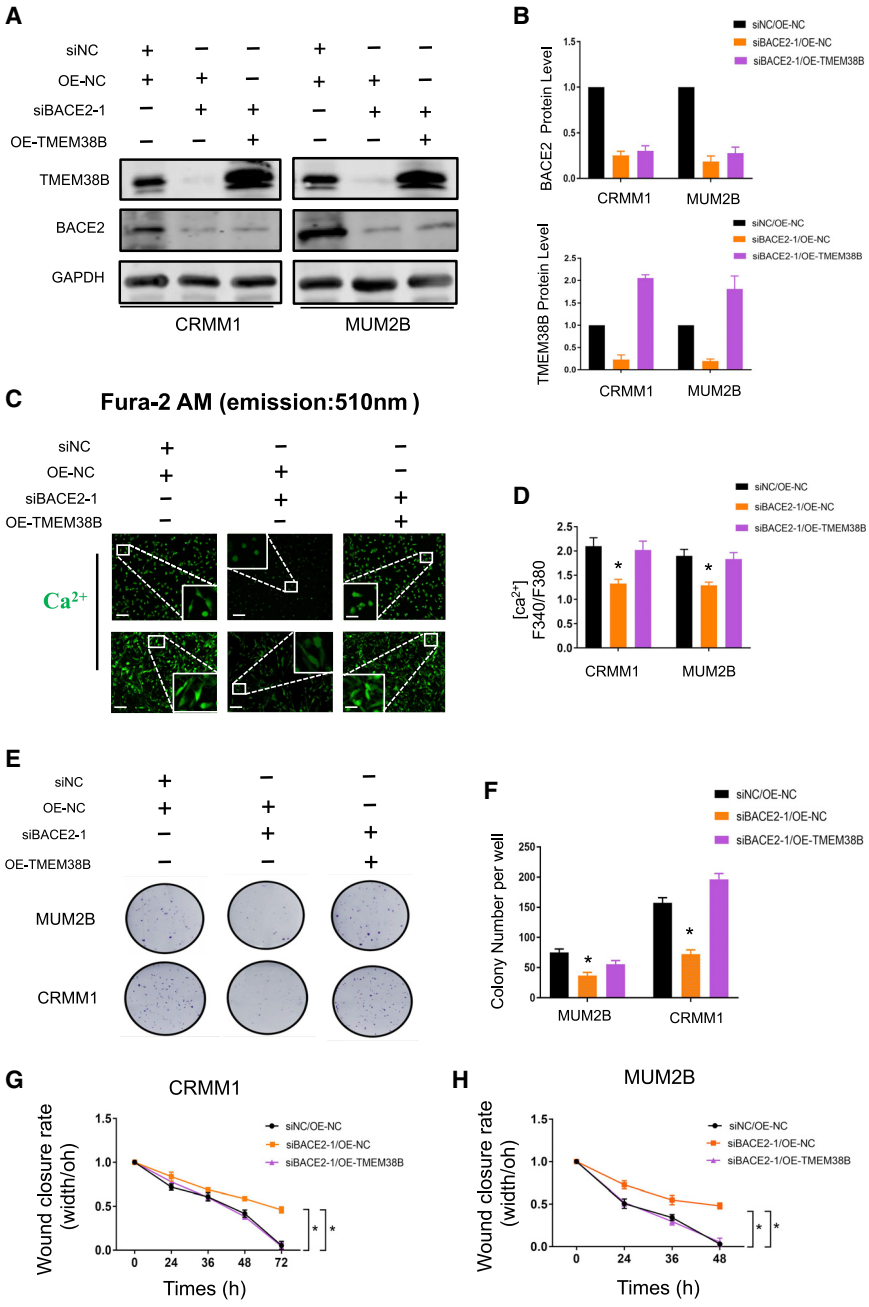

Figure 6. Reintroduction of TMEM38B rescued Ca^{2+} influx and the inhibitory phenotype

(A and B) Western blot showing the protein levels of TMEM38B and BACE2 in the BACE2-silenced cells before and after reintroduction of TMEM38B (A) and statistical results of TMEM38B and BACE2 expression (B). (C and D) Intracellular calcium concentration was detected by a calcium fluorescence probe (fura-2 AM) before and after reintroduction of TMEM38B in the BACE2-silenced cells. Scale bars, 100 μm (C). The fluorescence intensity of 60 s showed that the level of calcium ions increased significantly after reintroduction of TMEM38B. (E and F) A colony formation assay was used to assess the cell growth rate of tumor cells before and after reintroduction of TMEM38B in the BACE2-silenced cells (E). Statistical analysis of the colony formation assay performed using MUM2B and CRMM1 cells before and after reintroduction of TMEM38B in the BACE2-silenced cells, *$p < 0.05$ (F). (G and H) Wound-healing assay statistics demonstrate tumor migration. The results are expressed as the ratio of the current width to the original scratch width. *$p < 0.05$, compared with the control.

immunoprecipitation (meRIP) sequencing (meRIP-seq) (Figure 7A) and m^6A individual-nucleotide-resolution cross-linking and immunoprecipitation sequencing (miCLIP-seq) (Figure 7B) in ocular melanoma cells (GEO: GSE137675), we found that a part of the 3′ untranslated region (UTR) of BACE2 (hg19, chr21:42,648,297–42,648,500) was significantly enriched and presented a distinct peak in both meRIP-seq and miCLIP-seq data. We further validated that BACE2 mRNA was significantly hypermethylated through meRIP-quantitative polymerase chain reaction (qPCR) (Figure 7C). To determine the potential m^6A RNA methylation regulator of BACE2, we queried TCGA database and investigated the correlation between BACE2 expression and m^6A RNA methylation writers in UM patients. Herein, only methyltransferase like 3 (METTL3) showed significant positive correlation with BACE2 expression ($R = 0.3$, $p = 0.0076$) (Figures 7D and S13A). We next knocked down METTL3 through two individual shRNAs (Figure 7E, left panel). After silencing METTL3, we observed a significant decrease in methylated BACE2 RNA (Figure 7F) with decreased BACE2 expression at both the RNA (Figure S13B) and protein levels (Figure 7E, middle panel). In the enriched 3′ UTR of BACE2, we found three RRACH motifs, c.2266A (AGACT), c.2361A (AGACC), and c.2377A (GAACT), and mutated each A into T. We then cloned the corresponding wild-type and mutated 3′ UTRs into the pmirGLO vector (Figure 8A). The luciferase reporter gene assay demonstrated that c.A2266T presented a decreased signal, while the signals in other mutated groups remained unchanged (Figure 8B). Thus, m^6A RNA methylation of c.2266A in the 3′ UTR of BACE2 RNA contributed to the excessive expression in ocular melanoma.

DISCUSSION

BACE2, a transmembrane aspartic acid protease of the pepsin family, has been reported to be involved in the pathogenesis of several diseases.[15] For example, BACE2 was a dose-sensitive Alzheimer's disease

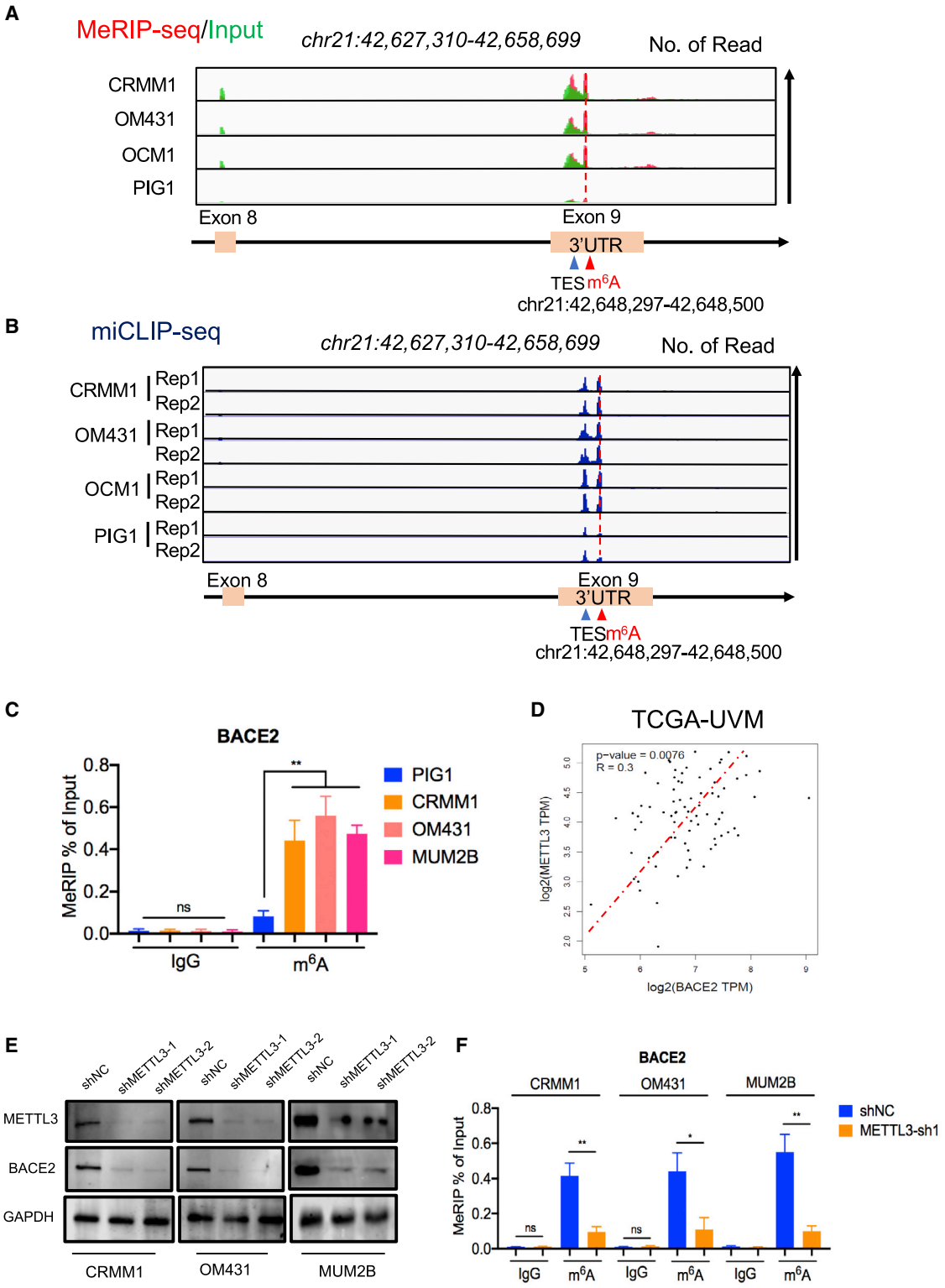

Figure 7. METTL3-mediated m^{6}A modification participated in the overexpression of BACE2 in ocular melanoma.

(A and B) IGV tracks displaying the meRIP-seq and miCLIP-seq read coverage of BACE2 in the normal and tumor cells. (C) meRIP-qPCR was performed to show that BACE2 mRNA was significantly hypermethylated in tumor cells. Error bars indicate the mean ± SEM (n = 3). **p < 0.01. ns, not significant. (D) Western blot showing

(legend continued on next page)

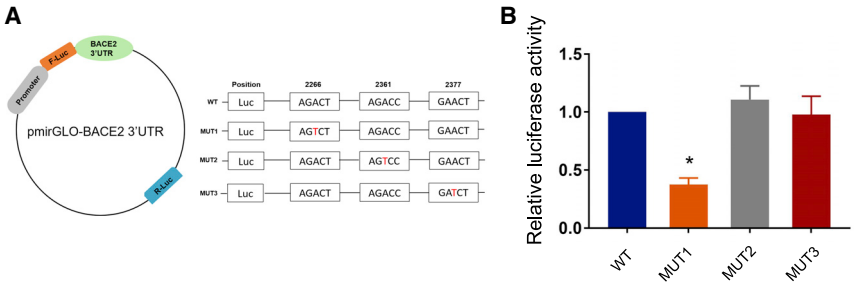

Figure 8. Wild-type BACE2 3′ UTR and BACE2 3′ UTR with a mutation at the m^{6}A consensus sequence were cloned into a luciferase reporter

(A) Mutations in the m6A modification region were generated by replacing adenosine with thymine. (B) The luciferase reporter gene assay demonstrated the relative luciferase activity of the wild-type and three mutant BATF2 3′ UTR reporter vectors. (C) Proposed mechanism of BACE2 in ocular melanoma. The m^{6}A modification of BACE mRNA by METTL3 improves its expression; BACE2 disrupts calcium homeostasis by promoting the expression of TMEM38B, which encodes a monovalent cation-specific channel and mediates Ca^{2+} release from intracellular stores.

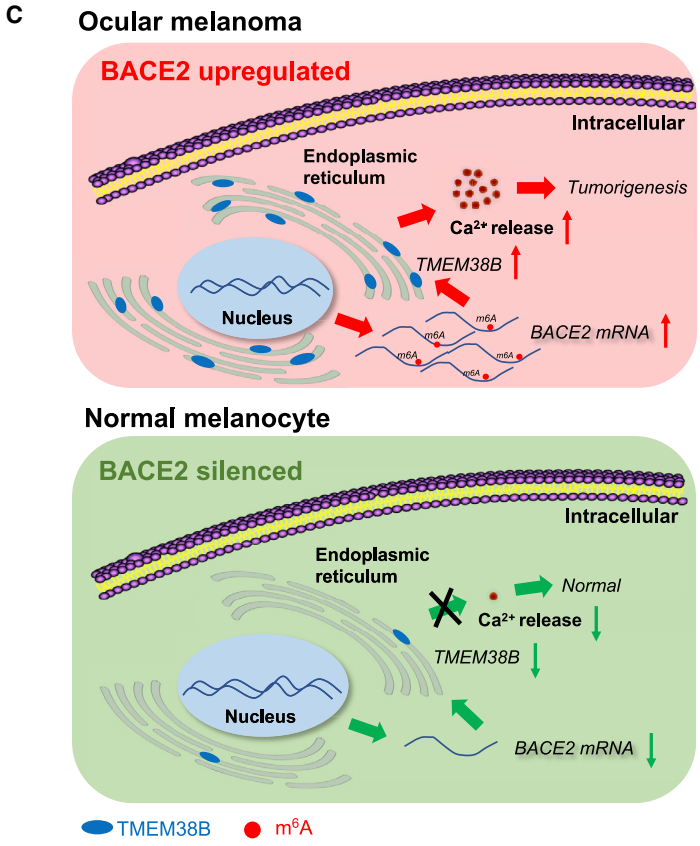

suppressor in human brain.[16] In type 2 diabetes, inhibition of BACE2 increased β cell mass and function and improved glucose tolerance by stabilizing Tmem27.[10] In addition, BACE2 facilitated protein aggregates to secrete into extracellular space, which in turn activated the YAP signaling cascade in metastatic melanoma.[17] However, the role of BACE2 in ocular melanoma remains unclear. In the present study, we first identified a link between intracellular calcium release and BACE2, which promoted ocular melanoma progression. By using *in vitro* and *in vivo* assays, we demonstrated that ocular melanoma exhibited high levels of BACE2, which activates its downstream gene TMEM38B to facilitate intracellular calcium release. In addition, BACE2/TMEM38B inhibition caused exhaustion of intracellular calcium release and effectively suppressed tumorigenesis. Our results revealed the carcinogenic effects of BACE2 in ocular melanoma, providing a novel understanding of the critical role of BACE2 in tumorigenesis (Figure 8C).

Dysfunctional calcium homeostasis is a key trigger and regulator of processes relevant to cancer, such as cell proliferation and migration.[18,19] For instance, the Orai1 and STIM1 proteins have been shown to participate in the influx of calcium from extracellular environment into cells, and reduction of these molecules decreased breast tumor cell migration, invasion, and metastasis.[20] In prostate cancer, endoplasmic reticulum (ER) TRPM8 was found to function as a Ca^{2+} release channel that promotes cancer progression.[21] In addition, several studies have revealed the role of Ca^{2+} homeostasis in melanoma tumor progression, and many molecular components of calcium-related pathways have been identified as interesting therapeutic targets.[22] Additionally, numerous Ca^{2+} channel genes, including TRPM2, TRPM7, and

the protein levels of METTL3 and BACE2 in the METTL3-silenced tumor cells. GAPDH was used as an internal control. (E) Reduction in m^{6}A modification in specific regions of BACE2 transcripts upon METTL3 knockdown, as assessed by gene-specific m^{6}A-RIP-qPCR assays, in CRMM1, OM431 and MUM2B cells. Error bars indicate the mean ± SEM (n = 3). *p < 0.05, **p < 0.01. (F) TCGA dataset showing METTL3 and BACE2 presented with parallel expression in uveal melanoma samples (p = 0.0076, R = 0.3).

TRPM8, were highly expressed in melanoma cells and increased tumor proliferation or favored metastasis and invasion.[23–25] In this study, we first identified the leading role of the BACE2/TMEM38B/Ca^{2+} pathway in the tumorigenesis of ocular melanoma. To the best of our knowledge, this is the first example of BACE2-mediated intracellular calcium release via TMEM38B contributing to ocular melanoma progression. To explore plausible mechanisms of how BACE2 regulates TMEM38B expression, we queried the STRING database to determine possible BACE2-interacting proteins. We found that BACE2 could potentially regulate several transcriptional factors, such as CTNNB1 (β-catenin) and CTNND1 (catenin delta 1) (Figure S14A), which translocated into nucleus and activated Wnt signaling during epithelial-mesenchymal transition.[26] We therefore speculate that BACE2 may regulate the transcription of TMEM38B through these transcriptional factors. The molecular mechanism underlying BACE2-guided TMEM38B transcriptional regulation remains investigation.

Ocular melanoma, mainly including UM and CM, is the most common eye malignancy in adults and has a poor prognosis.[27,28] Driver mutations of some genes, such as GNAQ and GNA11 in UM and BRAF and NRAS in CM, have been known for a long time.[29,30] Currently, important research efforts on epigenetic drivers have provided new insights into the molecular pathogenesis of ocular melanoma. Studies have shown that lncRNA ZNNT1 promoted autophagy by upregulating ATG12 to inhibit the tumorigenesis of UM.[31] Abnormal changes in DNA methylation, histone modification, and microRNAs were also observed in ocular melanoma.[32–34] In the present study, we demonstrated for the first time that BACE2 contributes to tumorigenesis and is a novel oncogene in ocular melanoma, thus furthering our understanding of ocular melanoma progression. Herein, we suggest that BACE2 is associated with poor prognosis among patients with ocular melanoma and acts as a potential therapeutic target for ocular melanoma.

m^6A RNA modification regulated by N^6-methyltransferases and demethylases is crucial for RNA processing, translation, and degradation, and aberrant m^6A levels cause tumor initiation and progression.[35] For instance, AURKA enhances oncogenic m^6A modification of DROSHA mRNA to improve its stability, contributing to breast cancer stem-like cell properties.[36] In ocular melanoma, targeted correction of aberrant m^6A exhibited therapeutic efficacy through translational activation of HINT2.[7] Moreover, cycloleucine, an m^6A RNA methylation inhibitor, triggered a significant tumor killing effect in ocular melanoma.[37] Our study showed that upregulation of BACE2 mRNA levels was a result of its increased m^6A RNA methylation level, thereby inducing tumorigenesis. Further research should focus on identifying other factors that may co-regulate BACE2 expression.

Notably, TMEM38B, encoding the ER membrane trimeric intracellular cation channel subtype B (TRIC-B), functions as a monovalent cation-specific channel mediating Ca^{2+} release from intracellular stores.[38] TMEM38B has been proven to be involved in numerous cellular functions, including perinatal lung maturation and bone mineralization.[39,40] Moreover, mutations in this gene may be associated with autosomal recessive osteogenesis imperfecta.[41,42] Thus far, there is no evidence suggesting that the TMEM38B gene plays a role in the development of ocular melanoma. Our data showed that TMEM38B was elevated in ocular melanoma and acted as a novel oncogene that promotes tumorigenesis.

In summary, our study initially elucidated a novel model of tumorigenesis in which BACE2, upregulated by the m^6A modification level, served as an oncogene and outlined a new pattern of intracellular calcium release regulation in ocular melanoma tumorigenesis, thus providing a novel therapeutic target for ocular melanoma therapy. Most importantly, understanding the various roles of intracellular calcium release in tumor progression inspired us to explore targeted correction of aberrant intracellular calcium release in disease treatment.

MATERIALS AND METHODS

Patient samples

A total of 47 human ocular melanoma tissues and 27 human normal melanocyte tissues were collected for immunofluorescence (IF) from patients of Shanghai Ninth People's Hospital, Shanghai JiaoTong University School of Medicine from 2007 to 2017. The histological features of all specimens were evaluated by independent pathologists, and the clinicopathological characteristics of the ocular melanoma patients are listed in Table S2.

Cell lines

The human ocular melanoma cell lines MUM2B and OM431 were kind gifts from Prof. John F. Marshall (Tumor Biology Laboratory, Cancer Research UK Clinical Center, John Vane Science Centre, London, UK). The MEL290, OMM1, OMM2.3 CRMM1, CRMM2, and CM2005.1 cell lines were kindly supplied by Prof. Martine J. Jager (Leiden University Medical Center, Leiden, the Netherlands). The PIG1 human normal melanocyte cell line was obtained from the Department of Ophthalmology, Peking University Third Hospital. The HEK293T human embryonic kidney cell line was purchased from the American Type Culture Collection (Manassas, VA, USA). The cell lines used in this study were authenticated by short tandem repeat (STR) profiling.

Cell culture

Human MUM2B, OM431, and HEK293T cells were cultured in DMEM (Gibco). PIG1, MEL290, OMM1, OMM2.3, and CM2005.1 were cultured in RPMI 1640 medium (Gibco). CRMM1 and CRMM2 cells were cultured in Ham's F-12K (Kaighn's) medium (Gibco). All media were supplemented with 10% certified heat-inactivated fetal bovine serum (FBS; Gibco), penicillin (100 U/mL), and streptomycin (100 mg/mL), and cells were all cultured at 37°C in a humidified 5% CO_2 atmosphere.

RNA isolation and quantitative real-time PCR

Total RNA was extracted from samples using the EZ-press RNA purification kit (B0004), and cDNA was generated using a PrimeScript

RT reagent kit (TaKaRa). Quantitative real-time PCR using PowerUp SYBR Green PCR master mix (Life Technologies) was performed using a real-time PCR system (Applied Biosystems). The primers used for real-time PCR in this study are listed in Table S1.

Plasmid construction, lentivirus packaging, and generation of stable cell lines

pLKO.1, pCDH, and pCMV were used in our study. shRNA sequences were generated by PCR and then cloned into the pLKO.1 vector. The TMEM38b overexpression cassette was generated by PCR and cloned into the pLvx-CMV-EGFP-Puro vector and verified by DNA sequencing. Lipofectamine 3000 reagent (Invitrogen) was incubated with Opti-MEM I reduced serum medium (Gibco), and HEK239T cells were transfected with 3 mg of plasmid or 6.0 mg of the PsPax plasmid. Eight hours after transfection, the medium was replaced with 10 mL of fresh medium. The supernatant containing the viruses was collected at 48 and 72 h, filtered through a 0.45-mm cellulose acetate filter, and used immediately. Viruses carrying a given plasmid were premixed 1:1, and 50 μL of virus was added to 1 mL of serum. Twenty-four hours prior to transfection, tumor cells were seeded at 2.0×10^5 cells per well in a 6-cm dish, and the medium was replaced with virus-containing supernatant supplemented with 10 ng/mL Polybrene (Sigma-Aldrich). After 48 h, the medium was replaced with fresh medium. Cells were selected by incubation with 4 mg/mL puromycin (InvivoGen) for 2 weeks and maintained in 1 mg/mL puromycin (InvivoGen).

Western blot

Cells were harvested at the indicated times and rinsed three times with PBS. Cell extracts were prepared with lysis buffer and centrifuged at 13,000 × *g* for 30 min at 4°C. Protein samples were separated by 7.5% (w/v) sodium dodecyl sulfate-polyacrylamide gel electrophoresis (SDS-PAGE) and transferred to polyvinylidene fluoride membranes. After blocking with 5% milk for 1 h at room temperature, the membrane was incubated with 2.5 μg/mL antibody in 5% BSA overnight at 4°C. The membrane was then incubated with a secondary antibody conjugated to a fluorescent tag (Invitrogen). Anti-BACE2 (1:500 dilution, Abcam), anti-GAPDH (#60004-1-Ig, 1:5,000 dilution, Proteintech), or anti-β-actin (#A5441, 1:5,000 dilution, Sigma-Aldrich, USA) was used. The band signals were visualized and quantified using the Odyssey infrared imaging system (LI-COR Biosciences, USA). Unmodified images are included in Supplemental information.

Cell proliferation assays and colony formation assays

Cell proliferation/growth was assessed by Cell Counting Kit-8 (CCK-8) assays (HY-K0301, MedChemExpress) following the manufacturer's instructions. Briefly, cells were seeded in triplicate in 96-well plates at a density of 2,000 cells/100 mL. Dye solution was added at the indicated time points, and the plates were incubated at 37°C for 3–4 h before the absorbance was detected at 570 nm. For the colony formation assay, a volume of 1 mL of complete medium containing 1,000 cells was placed in each well of a six-well plate. The plate was stained with 0.25% crystal violet after 1–2 weeks.

RNA extraction, library construction, Illumina sequencing (RNA-seq), and data analysis

Total RNA was extracted from samples using the EZ-press RNA purification kit (B0004). We confirmed the integrity of the RNA using a 2100 Bioanalyzer (Agilent Technologies, USA) and measured the RNA concentration using a Qubit 2.0 fluorometer with a Qubit RNA assay kit (Life Technologies, Carlsbad, CA, USA). We then prepared libraries from 100 ng of total RNA using the Illumina TruSeq RNA sample prep kit (Illumina, San Diego, CA, USA) following the manufacturer's protocol. Sequencing and basic informatics assays were performed by Aksomics.

Intracellular calcium release assay

The calcium transients were recorded as the 340/380 nm ratio (R) of the resulting 510-nm emissions, as previously described. The intracellular Ca^{2+} concentration ($[Ca^{2+}]_i$) was calculated using the equation $[Ca^{2+}]_i = K_d(R - R_{min})/(R_{max} - R)(F^{380}{}_{max}/F^{380}{}_{min})$, where R_{min} is the ratio at 0 Ca^{2+}, R_{max} is the ratio when fura-2 is completely saturated with Ca^{2+}, $F^{380}{}_{min}$ is the fluorescence at 380 nm for 0 Ca^{2+}, $F^{380}{}_{max}$ is the fluorescence at saturating Ca^{2+}, and the diffusion constant (K_d) = 224 nM. For stimulation of Ca^{2+} release, 200 μM adenosine triphosphate (ATP) was injected into cultures at 0 s. The intracellular calcium level was recorded at 0, 20, 40, 60, 80, and 100 s.

Statistical analyses

Data are presented as mean ± standard deviation (SD). Statistical analyses were performed using an unpaired Student's t test and one-way ANOVA followed by a Tukey's post-test in Prism 8.0 software (GraphPad, San Diego, CA, USA). $^*p < 0.05$, $^{**}p < 0.01$.

Availability of data and materials

The raw sequence data reported in this paper, including RNA-seq, miCLIP-seq, and meRIP-seq data, have been deposited in the Gene Expression Omnibus database (GEO: GSE137675), and also the Genome Sequence Archive in the Beijing Institute of Genomics (BIG) Data Center, Chinese Academy of Sciences, under accession no. CRA001675 (https://bigd.big.ac.cn/gsa/s/n110138p), and are publicly accessible at https://bigd.big.ac.cn/gsa. In addition, RNA-seq of BACE2-silenced cells have been uploaded in the Gene Expression Omnibus database (GEO: GSE155530).

Ethics approval and consent to participate

This research was performed in accordance with the World Medical Association Declaration of Helsinki. Written informed consent was obtained from all patients. The study was approved by the Ethics Committee of Shanghai JiaoTong University.

SUPPLEMENTAL INFORMATION

Supplemental Information can be found online at https://doi.org/10.1016/j.ymthe.2021.02.014.

ACKNOWLEDGMENTS

We thank all the uveal melanoma and conjunctival melanoma patients enrolled in our study and wish them good health. This work

was supported by the National Key Research and Development Plan (grant 2018YFC1106100), the National Natural Science Foundation of China (grants 81772875, 81872339, and 81802702), the China Postdoctoral Science Foundation funded project (2020M681328), and by the Science and Technology Commission of Shanghai (17DZ2260100 and 19JC1410200).

AUTHOR CONTRIBUTIONS

R.J., P.C., and X.X. designed the research, supervised the experiments, and approved the manuscript. F.H. performed the experiments with assistance from J. Yu, J. Yang, A.Z., and H.S.; X.G. and S.W. performed the bioinformatics analyses and contributed to the experimental candidate selection; P.C. and F.H. analyzed the data and drafted the manuscript. X.X. and R.J. were responsible for sample collection. All the authors read and approved this manuscript.

DECLARATION OF INTERESTS

The authors declare no competing interests.

REFERENCES

1. Pelster, M.S., Gruschkus, S.K., Bassett, R., Gombos, D.S., Shephard, M., Posada, L., Glover, M.S., Simien, R., Diab, A., Hwu, P., et al. (2020). Nivolumab and ipilimumab in metastatic uveal melanoma: results from a single-arm phase II study. J. Clin. Oncol. Published online October 30, 2020.
2. Moore, A.R., Ran, L., Guan, Y., Sher, J.J., Hitchman, T.D., Zhang, J.Q., Hwang, C., Walczak, E.G., Shoushtari, A.N., Monette, S., et al. (2020). GNA11 Q209L mouse model reveals RasGRP3 as an essential signaling node in uveal melanoma. Cell Rep. *33*, 108277.
3. Boru, G., Cebulla, C.M., Sample, K.M., Massengill, J.B., Davidorf, F.H., and Abdel-Rahman, M.H. (2019). Heterogeneity in mitogen-activated protein kinase (MAPK) pathway activation in uveal melanoma with somatic *GNAQ* and *GNA11* mutations. Invest. Ophthalmol. Vis. Sci. *60*, 2474–2480.
4. Chen, X., Wu, Q., Depeille, P., Chen, P., Thornton, S., Kalirai, H., Coupland, S.E., Roose, J.P., and Bastian, B.C. (2017). RasGRP3 mediates MAPK pathway activation in GNAQ mutant uveal melanoma. Cancer Cell *31*, 685–696.e6.
5. Sagiv, O., Thakar, S.D., Kandl, T.J., Ford, J., Sniegowski, M.C., Hwu, W.J., and Esmaeli, B. (2018). Immunotherapy with programmed cell death 1 inhibitors for 5 patients with conjunctival melanoma. JAMA Ophthalmol. *136*, 1236–1241.
6. Wang, Y., Su, L., Morin, M.D., Jones, B.T., Mifune, Y., Shi, H., Wang, K.W., Zhan, X., Liu, A., Wang, J., et al. (2018). Adjuvant effect of the novel TLR1/TLR2 agonist Diprovocim synergizes with anti-PD-L1 to eliminate melanoma in mice. Proc. Natl. Acad. Sci. USA *115*, E8698–E8706.
7. Jia, R., Chai, P., Wang, S., Sun, B., Xu, Y., Yang, Y., Ge, S., Jia, R., Yang, Y.G., and Fan, X. (2019). m^6A modification suppresses ocular melanoma through modulating HINT2 mRNA translation. Mol. Cancer *18*, 161.
8. Fan, J., Xing, Y., Wen, X., Jia, R., Ni, H., He, J., Ding, X., Pan, H., Qian, G., Ge, S., et al. (2015). Long non-coding RNA ROR decoys gene-specific histone methylation to promote tumorigenesis. Genome Biol. *16*, 139.
9. Tang, J., Wan, Q., and Lu, J. (2020). The prognostic values of m6A RNA methylation regulators in uveal melanoma. BMC Cancer *20*, 674.
10. Esterházy, D., Stützer, I., Wang, H., Rechsteiner, M.P., Beauchamp, J., Döbeli, H., Hilpert, H., Matile, H., Prummer, M., Schmidt, A., et al. (2011). Bace2 is a β cell-enriched protease that regulates pancreatic β cell function and mass. Cell Metab. *14*, 365–377.
11. Wang, Z., Xu, Q., Cai, F., Liu, X., Wu, Y., and Song, W. (2019). BACE2, a conditional β-secretase, contributes to Alzheimer's disease pathogenesis. JCI Insight *4*, e123431.
12. Rochin, L., Hurbain, I., Serneels, L., Fort, C., Watt, B., Leblanc, P., Marks, M.S., De Strooper, B., Raposo, G., and van Niel, G. (2013). BACE2 processes PMEL to form the melanosome amyloid matrix in pigment cells. Proc. Natl. Acad. Sci. USA *110*, 10658–10663.
13. Tang, Z., Li, C., Kang, B., Gao, G., Li, C., and Zhang, Z. (2017). GEPIA: a web server for cancer and normal gene expression profiling and interactive analyses. Nucleic Acids Res. *45* (W1), W98–W102.
14. Ali, E.S., Rychkov, G.Y., and Barritt, G.J. (2020). Targeting Ca^{2+} signaling in the initiation, promotion and progression of hepatocellular carcinoma. Cancers (Basel) *12*, 2755.
15. Lin, X., Koelsch, G., Wu, S., Downs, D., Dashti, A., and Tang, J. (2000). Human aspartic protease memapsin 2 cleaves the β-secretase site of β-amyloid precursor protein. Proc. Natl. Acad. Sci. USA *97*, 1456–1460.
16. Alić, I., Goh, P.A., Murray, A., Portelius, E., Gkanatsiou, E., Gough, G., Mok, K.Y., Koschut, D., Brunmeir, R., Yeap, Y.J., et al.; LonDownS Consortium (2020). Patient-specific Alzheimer-like pathology in trisomy 21 cerebral organoids reveals BACE2 as a gene dose-sensitive AD suppressor in human brain. Mol. Psychiatry. Published online July 10, 2020.
17. Matafora, V., Farris, F., Restuccia, U., Tamburri, S., Martano, G., Bernardelli, C., Sofia, A., Pisati, F., Casagrande, F., Lazzari, L., et al. (2020). Amyloid aggregates accumulate in melanoma metastasis modulating YAP activity. EMBO Rep. *21*, e50446.
18. Azimi, I., Roberts-Thomson, S.J., and Monteith, G.R. (2014). Calcium influx pathways in breast cancer: opportunities for pharmacological intervention. Br. J. Pharmacol. *171*, 945–960.
19. Gao, Y., and Liao, P. (2019). TRPM4 channel and cancer. Cancer Lett. *454*, 66–69.
20. Tsai, F.C., Seki, A., Yang, H.W., Hayer, A., Carrasco, S., Malmersjö, S., and Meyer, T. (2014). A polarized Ca^{2+}, diacylglycerol and STIM1 signalling system regulates directed cell migration. Nat. Cell Biol. *16*, 133–144.
21. Bidaux, G., Flourakis, M., Thebault, S., Zholos, A., Beck, B., Gkika, D., Roudbaraki, M., Bonnal, J.L., Mauroy, B., Shuba, Y., et al. (2007). Prostate cell differentiation status determines transient receptor potential melastatin member 8 channel subcellular localization and function. J. Clin. Invest. *117*, 1647–1657.
22. Macià, A., Herreros, J., Martí, R.M., and Cantí, C. (2015). Calcium channel expression and applicability as targeted therapies in melanoma. BioMed Res. Int. *2015*, 587135.
23. Orfanelli, U., Wenke, A.K., Doglioni, C., Russo, V., Bosserhoff, A.K., and Lavorgna, G. (2008). Identification of novel sense and antisense transcription at the TRPM2 locus in cancer. Cell Res. *18*, 1128–1140.
24. Chen, J.P., Luan, Y., You, C.X., Chen, X.H., Luo, R.C., and Li, R. (2010). TRPM7 regulates the migration of human nasopharyngeal carcinoma cell by mediating Ca^{2+} influx. Cell Calcium *47*, 425–432.
25. Yamamura, H., Ugawa, S., Ueda, T., Morita, A., and Shimada, S. (2008). TRPM8 activation suppresses cellular viability in human melanoma. Am. J. Physiol. Cell Physiol. *295*, C296–C301.
26. Han, L., Li, Z., Jiang, Y., Jiang, Z., and Tang, L. (2019). SNHG29 regulates miR-223-3p/CTNND1 axis to promote glioblastoma progression via Wnt/β-catenin signaling pathway. Cancer Cell Int. *19*, 345.
27. Kujala, E., Mäkitie, T., and Kivelä, T. (2003). Very long-term prognosis of patients with malignant uveal melanoma. Invest. Ophthalmol. Vis. Sci. *44*, 4651–4659.
28. Zhou, C., Wang, Y., Jia, R., and Fan, X. (2017). Conjunctival melanoma in Chinese patients: local recurrence, metastasis, mortality, and comparisons with Caucasian patients. Invest. Ophthalmol. Vis. Sci. *58*, 5452–5459.
29. Jager, M.J., Shields, C.L., Cebulla, C.M., Abdel-Rahman, M.H., Grossniklaus, H.E., Stern, M.H., Carvajal, R.D., Belfort, R.N., Jia, R., Shields, J.A., and Damato, B.E. (2020). Uveal melanoma. Nat. Rev. Dis. Primers *6*, 24.
30. Zeng, Y., Hu, C., Shu, L., Pan, Y., Zhao, L., Pu, X., and Wu, F. (2020). Clinical treatment options for early-stage and advanced conjunctival melanoma. Surv. Ophthalmol. Published online September 25, 2020.
31. Li, P., He, J., Yang, Z., Ge, S., Zhang, H., Zhong, Q., and Fan, X. (2020). *ZNNT1* long noncoding RNA induces autophagy to inhibit tumorigenesis of uveal melanoma by regulating key autophagy gene expression. Autophagy *16*, 1186–1199.
32. Robertson, A.G., Shih, J., Yau, C., Gibb, E.A., Oba, J., Mungall, K.L., Hess, J.M., Uzunangelov, V., Walter, V., Danilova, L., et al.; TCGA Research Network (2017). Integrative analysis identifies four molecular and clinical subsets in uveal melanoma. Cancer Cell *32*, 204–220.e15.

33. Li, Y., Jia, R., and Ge, S. (2017). Role of epigenetics in uveal melanoma. Int. J. Biol. Sci. *13*, 426–433.

34. Larsen, A.C., Mikkelsen, L.H., Borup, R., Kiss, K., Toft, P.B., von Buchwald, C., Coupland, S.E., Prause, J.U., and Heegaard, S. (2016). MicroRNA expression profile in conjunctival melanoma. Invest. Ophthalmol. Vis. Sci. *57*, 4205–4212.

35. Wang, S., Chai, P., Jia, R., and Jia, R. (2018). Novel insights on m^6A RNA methylation in tumorigenesis: a double-edged sword. Mol. Cancer *17*, 101.

36. Peng, F., Xu, J., Cui, B., Liang, Q., Zeng, S., He, B., Zou, H., Li, M., Zhao, H., Meng, Y., et al. (2020). Oncogenic AURKA-enhanced N^6-methyladenosine modification increases *DROSHA* mRNA stability to transactivate *STC1* in breast cancer stem-like cells. Cell Res. Published online August 28, 2020.

37. Luo, G., Xu, W., Zhao, Y., Jin, S., Wang, S., Liu, Q., Chen, X., Wang, J., Dong, F., Hu, D.N., et al. (2020). RNA m^6A methylation regulates uveal melanoma cell proliferation, migration, and invasion by targeting c-Met. J. Cell. Physiol. *235*, 7107–7119.

38. Hu, Z., and Gulyaeva, O. (2019). TRIC-B: an under-explored druggable ion channel. Nat. Rev. Drug Discov. *18*, 657.

39. Yamazaki, D., Komazaki, S., Nakanishi, H., Mishima, A., Nishi, M., Yazawa, M., Yamazaki, T., Taguchi, R., and Takeshima, H. (2009). Essential role of the TRIC-B channel in Ca^{2+} handling of alveolar epithelial cells and in perinatal lung maturation. Development *136*, 2355–2361.

40. Zhao, C., Ichimura, A., Qian, N., Iida, T., Yamazaki, D., Noma, N., Asagiri, M., Yamamoto, K., Komazaki, S., Sato, C., et al. (2016). Mice lacking the intracellular cation channel TRIC-B have compromised collagen production and impaired bone mineralization. Sci. Signal. *9*, ra49.

41. Shaheen, R., Alazami, A.M., Alshammari, M.J., Faqeih, E., Alhashmi, N., Mousa, N., Alsinani, A., Ansari, S., Alzahrani, F., Al-Owain, M., et al. (2012). Study of autosomal recessive osteogenesis imperfecta in Arabia reveals a novel locus defined by *TMEM38B* mutation. J. Med. Genet. *49*, 630–635.

42. Volodarsky, M., Markus, B., Cohen, I., Staretz-Chacham, O., Flusser, H., Landau, D., Shelef, I., Langer, Y., and Birk, O.S. (2013). A deletion mutation in TMEM38B associated with autosomal recessive osteogenesis imperfecta. Hum. Mutat. *34*, 582–586.